J Therm Anal Calorim (2015) 121:309–318
DOI 10.1007/s10973-015-4532-1

Pyrolysis, combustion and oxy-combustion studies of sugarcane industry wastes and its blends

Daniel R. da Silva · Marisa S. Crespi · Paula C. G. M. Crnkovic · Clovis A. Ribeiro

Received: 7 October 2014 / Accepted: 2 February 2015 / Published online: 3 March 2015

Abstract The aim of this work was on the thermal characterization of wastes of the sugarcane industry, such as bagasse, filter cake and vinasse, in both forms: pure and blended. Thermogravimetric analysis (TG), derivative thermogravimetric (DTG) and differential thermal analysis (DTA) were used for the evaluation of the thermal behavior of the samples under four different atmospheres: N_2, CO_2, N_2/O_2 and CO_2/O_2. Comparison of thermal behavior of the samples under combustion (N_2/O_2) and oxy-combustion (CO_2/O_2) reveals that replacing N_2 by CO_2 causes displacement of mass loss steps to higher temperatures and increases some DTG peaks. Higher heat capacity of carbon dioxide and higher partial pressure of CO_2 molecules in relation to N_2 ones explain these observations. Under CO_2 (100 %) environment, an endothermic event—due to CO release—is observed at around 900 °C, which is attributed to the reverse Boudouard reaction. Interestingly, in all samples, when vinasse is present, such endothermic event starts at lower temperature (~700 °C), which can be understood as a reaction catalyzed by the high potassium content in the vinasse. Synergistic effect studies indicated that bagasse improved reactivity of blends due to its higher volatile content. Since there are no reports regarding the thermal characterization of wastes of the sugarcane industry under combustion, oxy-combustion and gasification atmospheres, this work establishes an important database for the study of similar types of biomass in the field of bioenergy.

Keywords Bagasse · Vinasse · Filter cake · Thermal analysis · Oxy-combustion · Gasification

D. R. da Silva · M. S. Crespi · P. C. G. M. Crnkovic · C. A. Ribeiro (✉)
Institute of Chemistry, São Paulo State University (UNESP), R. Prof. Francisco Degni 55, Araraquara, SP, Brazil
e-mail: ribeiroc@iq.unesp.br

P. C. G. M. Crnkovic
University of São Paulo (USP), Av. Trabalhador São-carlense 400, São Carlos, SP, Brazil

Introduction

The energetic demand is increasing due to population growth and industrialization. Conventional energy sources have limited reserves and should not last much longer [1]. It is estimated that current reserves of coal, oil and natural gas will last for another 218 years, 41 years and 63 years, respectively, if the present demand remains constant [2–4].

There are several promising solutions to decrease greenhouse gas emissions and further increasing energy efficiency. New technologies have been proposed to reduce CO_2 emissions, such as oxy-fuel combustion. In this process, the fuel is burnt in a rich oxygen environment and the recycling process provides the increasing of the CO_2 concentration, ready to be trapped [5].

The use of biomass in the oxy-fuel combustion process could be considered as the sink for CO_2 [6]. However, many technical and scientific features must be elucidated since it is a relatively new field of energy generation [7]. A plentiful biomass in Brazil is sugarcane and the wastes generated by sugarcane mills. Bagasse and filter cake are solid by-products of sugar and ethanol production [8]. Vinasse is a liquid waste from alcoholic fermentation of sugarcane juice for ethanol production [9].

The use of bagasse as a fuel depends on its heating capacity, which is consequence of its physical–chemical composition. Energy generation from bagasse is well established for decades in Brazil. Vinasse and filter cake

have been usually applied as fertilizers on sugarcane crops due to their high concentration of phosphorous and potassium [10]. However, such activity might cause several changes in soil such as elevation of pH, salinization and leaching of metals to underground waters [11, 12]. An alternative use of these wastes is anaerobic digestion for biogas generation [13]. Despite promising results, this process still presents some drawbacks like production of corrosive gases such as H_2S [14].

The incomplete combustion of biomass generates substantial amounts of several pollutants such as CO and particulate matter [15]. Furthermore, low efficiency of the process, ash sinterization and fouling in addition to large quantities of ashes produced by some biomasses are problems regarding this process [16]. Also, biomass presents lower amounts of carbon, lower heating values and higher contents of oxygen in relation to fossil fuels [13]. Finally, the presence of alkali metals and chlorine in biomass may derail the use of produced ashes in construction materials [17]. Chlorine present in the ashes interacts with alkali metals, enhancing their mobility by the generation of alkali chlorides with low melting points. Such compounds leave the ashes as volatile gases that cause direct corrosion by accelerating the oxidation of metal alloys [18, 19].

Co-firing of coal and biomass blends is one of the most promising alternatives to use renewable fuels due to high efficiency and low financial investment of the process. Since biomass and coal present quite different composition, such technique reduces CO_2, NO_x and SO_x emission levels in relation to coal-fired power plants [20]. Also, it minimizes wastes generation and decreases fuel costs, soil and water pollution. The existing coal power plants could be used for such purpose [21, 22]. Besides, the catalytic role of alkali and alkaline earth metals on pyrolysis and gasification of carbon is known for decades. Sodium and, mainly, potassium present higher catalytic activity among these metals [23–26]. Several reports related to the gasification of coal/biomass blends noticed such catalytic effect when a biomass rich in Na or K was employed [27–29].

Regarding biomass/biomass blends, Gil et al. [30] studied the combustion characteristics of pellets prepared from several sources of biomass (pine, chestnut and eucalyptus sawdust, cellulose residue, coffee husks and grape waste), pure and blended. They detected intermediate combustion profiles for the blends in relation to the raw samples by TG–DTG. Lajiji et al. [31] observed similar trends of thermal behavior for pellets constituted by blends of pine sawdust and olive waste in N_2 and synthetic air. Also, the authors noticed that, by adding olive waste to pine sawdust, the reactivity of the blend was improved due to higher volatile content of olive waste. Jirícek et al. [32], when burning biomass blends, observed that the addition of lignin (20–40 % ratio) to wheat straw modified volatilization rates, which affected oxidation, in an air–oxygen atmosphere by TG. Also, heat was released more continuously when co-firing lignin and wheat straw.

However, burning blends containing different sources of biomass are an important and promising field on pyrolysis, combustion and oxy-combustion processes. This study evaluated the thermal behavior of bagasse, filter cake, vinasse and their blends in typical atmospheres of pyrolysis, combustion and oxy-combustion. Some of the studied samples were also heated in a typical gasification atmosphere, and their thermal degradation profiles were investigated. Synergism between constituents of a blend was determined in order to estimate the interactions among volatiles and produced char during thermal decomposition.

Experimental

Sample preparation

Bagasse, filter cake and vinasse were obtained from sugarcane mills situated near Araraquara city (−21°47′40″S, 48°10′32″W, elevation of 664 m), São Paulo state, Brazil. The sugarcane plants (*Saccharum officinarum*) were harvested at an age of 12 months, approximately. They were milled in sugarcane mills, removing the juice out of the shredded pulp (bagasse), which was used in this study. The juice, after several steps, generates, as by-products, filter cake (from sugar production) and vinasse (from ethanol production).

All samples were prepared by washing with distilled water at room temperature (except vinasse) and drying at 80 °C to remove moisture. Then, they were ground or milled by a hand mortar followed by sieving to obtain particles with dimensions around 90 μm. For thermal characterization, the samples were mixed (1:1 w/w) in order to compare with original samples forming the following binary blends: bagasse + filter cake (B + Fc), bagasse + vinasse (B + V) and filter cake + vinasse (Fc + V).

In order to verify the occurrence of a catalytic effect of potassium on the reverse Boudouard reaction by thermal analysis, this metal was added to demineralized bagasse according to the procedure described by Jones et al. [33] with some adaptations. A mass of milled bagasse was heated to 60 °C for 5 h in 500 mL of HCl 2 mol L^{-1} under stirring. Then, the sample was filtered and washed in order to remove chloride ions. The demineralized bagasse was dried at 60 °C until no variation of mass was detected. A solution of 1 % potassium biphthalate was added to the sample, and the system was kept under stirring at room temperature for a week. Finally, the obtained K-enriched bagasse was filtered and dried.

Sample digestion

A mass of 1.00 g of original samples was digested in a 2012 Digestor FOSS Tecator® according to the procedure proposed by Jesus et al. [34]. A volume of 10.0 mL of concentrated HNO_3 was added to each sample, and the flasks were kept covered for 16 h at room temperature. Then, they were heated at 140 °C until total vaporization of the solvent. Another 10.0 mL of concentrated HNO_3 was added, and a 30 % H_2O_2 solution was slowly dropped into the reaction tubes until evolution of nitrous fumes ceased, resulting in a colorless solution which indicated the ending of digestion procedure.

The digested samples were cooled at room temperature, filtered and diluted in volumetric flasks (100 mL). They were stored in refrigerator for the determination of inorganic matter by: flame photometry (Micronal® B262 Flame Photometer)—Na and K; atomic absorption spectrophotometry (Varian® SpectrAA 240 FS)—Al, Ca, Fe and Mg; vis-spec (Femto® 435 spectrophotometer)—P.

FT-IR spectra

FT-IR spectra of samples were acquired by using a Perkin-Elmer® Spectrum 2000 spectrophotometer. The pellets were made by mixing each biomass sample with KBr at a 10:1 (m/m) ratio. The obtained spectrum for each sample was the average of 16 scans in the IR range of 4000–400 cm^{-1} at 2-cm^{-1} spectral resolution.

Thermal characterization

Thermogravimetric, derivative thermogravimetric and differential thermal analysis (TG, DTG and DTA, respectively) were performed by a TA Instruments® SDT-2960 Simultaneous DTA/DTG. For pyrolysis, combustion and oxy-combustion studies, N_2, synthetic air and CO_2/O_2 (8:2 v/v) atmospheres were employed at a flow of 100 mL min^{-1}. Also, thermal behavior of bagasse, vinasse, B + Fc blend and K-enriched bagasse in CO_2 atmosphere was studied. Mass of 6.0 ± 0.5 mg of each sample was heated from room temperature to 600 °C at a 20 °C min^{-1} rate. When CO_2 atmosphere was employed, samples were heated from room temperature to 1000 °C (1100 °C when K-enriched bagasse was employed) at a heating rate 30 °C min^{-1}.

Differential scanning calorimetry (DSC) analysis was performed by a TA Instruments® DSC 2910. Sample mass of 3.0 ± 0.5 mg was heated from room temperature to 600 °C at a 20 °C min^{-1} rate in static air atmosphere.

Evaluation of synergistic effect

In order to determine whether a synergistic effect between blend constituents actually occurred, an experimental DTG curve of that blend was compared to an estimated one, which was plotted as a sum of mass loss rates of each constituent of the blend according to the following equation (Eq. 1) [35]:

$$(dm/dT)_{AB} = X_A(dm/dT)_A + X_B(dm/dT)_B \quad (1)$$

where $(dm/dT)_A$ and $(dm/dT)_B$ are the mass loss rates of blend constituents (A and B) of the blend AB and X_A and X_B are their mass fractions. In this study, only binary blends (1:1 m/m ratio) were used; therefore, $X_A = X_B = 0.5$.

Results and discussion

Sample composition

As shown in Table 1, high concentrations of sodium and potassium were detected in vinasse, according to many reports regarding the use of that waste as a fertilizer [8, 36]. Due to its high phosphorous content, filter cake can also be employed for that purpose as well [37]. Although its ashes have been applied to soil fertilization [38], bagasse showed the lowest concentrations of those elements when compared to the other samples.

Regarding other elements, filter cake presented high concentration of Al and Fe. Vinasse presented a great concentration of Mg and Na. The high Ca concentration observed in both samples was due to the addition of $Ca(OH)_2$ to the juice for the production of sugar and ethanol.

FT-IR

Data acquired by FT-IR (Fig. 1) revealed that, as expected, all studied samples had similar organic composition.

Table 1 Element concentrations in dry samples

Chemical element	Concentration/g kg^{-1} (dry basis)		
	Bagasse	Filter cake	Vinasse
Al	0.276 ± 0.049	8.141 ± 0.084	0.804 ± 0.020
Ca	0.415 ± 0.028	15.50 ± 1.752	22.90 ± 1.997
Fe	0.403 ± 0.021	12.33 ± 0.311	1.477 ± 0.008
K	0.995 ± 0.070	4.406 ± 0.474	0.110 ± 0.058[a]
Mg	0.275 ± 0.011	2.196 ± 0.137	8.547 ± 0.027
Na	0.522 ± 0.065	1.272 ± 0.122	21.90 ± 1.058
P	0.127 ± 0.003	3.718 ± 0.693	1.901 ± 0.092

[a] $\times 10^3$

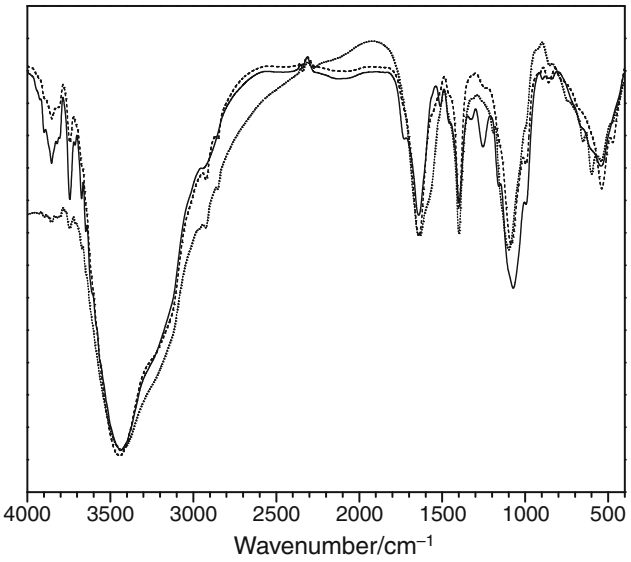

Fig. 1 FT-IR spectra of bagasse (*line*), filter cake (*dashed line*) and vinasse (*dotted line*)

Stretchings and scissorings related to carbonyl and hydroxyl functional groups were observed. Also, C–C and C–H stretchings associated with aromatic rings and aliphatic chains, respectively, typical of any biomass [39] were detected. Interpretation of the spectra is discussed in Table 2.

Thermal behavior of the samples

TG curves of the original samples are shown in Fig. 2. All samples presented moisture loss ($T < 150$ °C) and decomposition of organic matter in three steps of mass loss. Higher ash contents detected for filter cake and vinasse (47 and 40 %, respectively) in relation to bagasse (5 %). Also, vinasse started to decompose at a lower temperature than other samples, probably due to the absence of fibers in its structure, which favored degradation of the organic content. Furthermore, TG curves for the blends showed an intermediate trend in comparison with pure samples in every studied atmosphere. An intermediate thermal behavior in N_2/O_2 and CO_2/O_2 environments was also observed for all blends since they were constituted in a 1:1 mass ratio.

Figures 3 and 4 display the TG curves obtained for the pure samples in synthetic air and CO_2/O_2 atmospheres, respectively. In both conditions, vinasse showed the same trend as previously observed in N_2: sample decomposition started early (around 160 °C in synthetic air and CO_2/O_2) in comparison with bagasse and filter cake (above 250 °C in same conditions).

Also, from DTG curves, it was noticed that all studied samples presented four mass loss steps: First, there was moisture loss until 150 °C approximately; then, it was observed a peak with a shoulder at 310 °C regarding to hemicellulose and cellulose decomposition steps; finally, a peak at $T > 500$ °C emerged, related to degradation of the remaining lignin. Presence of CO_2 in the furnace atmosphere caused a displacement of the mass loss steps to higher temperatures for all samples.

Although a displacement of DTG peaks to higher temperatures was noticed, their intensities were increased for some samples in CO_2/O_2 atmosphere. Partial pressure of CO_2 affected the release of gaseous products, making such reactions faster than in N_2/O_2. Figure 5 shows a comparison between DTG curves in both atmospheres of bagasse.

DTA peaks (mainly the last one) were also displaced to higher temperatures in CO_2/O_2 (Fig. 6). Such feature was more pronounced in B + V and Fc + V blends. Furthermore, the intensity of DTA peaks was increased for some samples. Figure 6a, b compares DTA curves of B + V and Fc + V blends, respectively, in both atmospheres.

Table 2 Interpretation of FT-IR spectra of samples

Wavenumber/cm^{-1}	Attribution
4000–3600	O–H stretching (free phenols and alcohols)
3600–3400	N–H asymmetric stretching
3400–3100	C–H stretching of $=CH_2$
3000–2900	C–H stretching of –CH (methyl and methylene)
1800–1700	C=O stretching (non-conjugated ketones, carbonyl and esters)
1700–1600	C=O stretching (aromatic and p-substituted ketones)
1600–1550	C=O stretching coupled with aromatic rings vibrations
1550–1500	Aromatic rings vibrations
1500–1450	C–H asymmetric deformation ($–CH_3$ and $–CH_2$)
1450–1400	Aromatic rings vibrations coupled with C–H scissoring
1400–1300	C–H stretching (aliphatic C–H of CH_3 and phenolic O–H)
1300–1200	Condensation of S and G rings
1150–1100	C=O deformation (conjugated esters)
1100–1000	C–O deformation (secondary alcohols and aliphatic esters)
1000–950	C–H rocking (aromatic C–H), C–O deformation (primary alcohols) and C–H stretching
950–900	C–H angular deformation (CH sp)
900–850	C–H angular deformation (aromatic rings)
850–800	C–H angular deformation (G unit)
800–750	CH_2 vibration
650–600	OH angular deformation
600–500	C–C planar deformation
500–450	C–Cl angular deformation

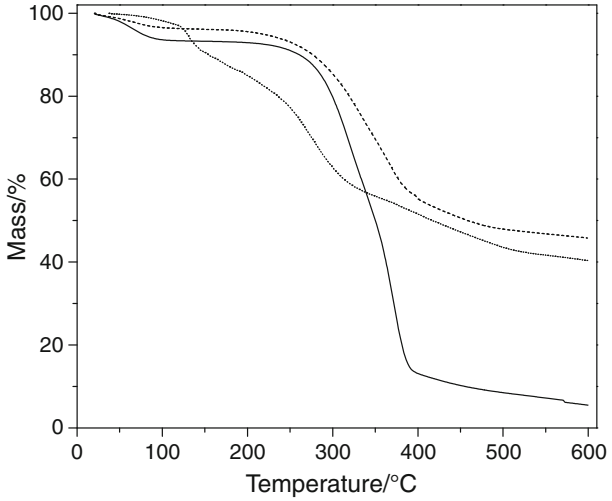

Fig. 2 TG curves in N_2 of bagasse (*line*), filter cake (*dashed line*) and vinasse (*dotted line*)

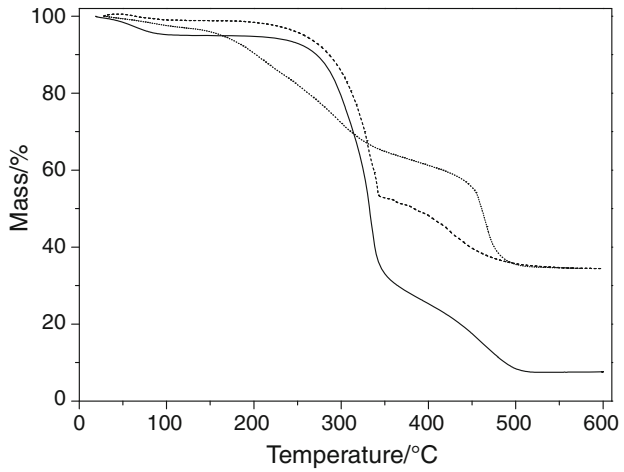

Fig. 3 TG curves in synthetic air of bagasse (*line*), filter cake (*dashed line*) and vinasse (*dotted line*)

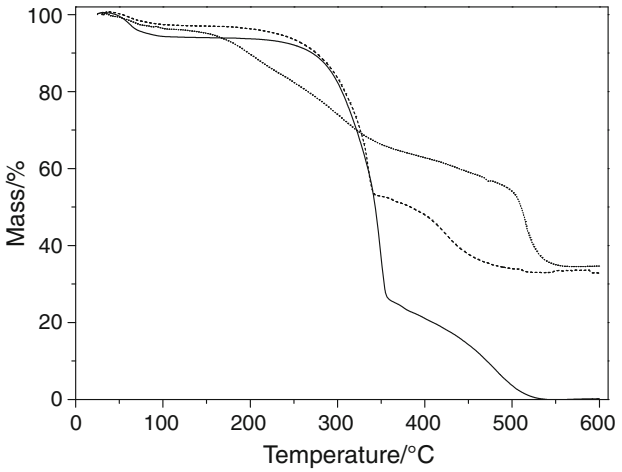

Fig. 4 TG curves in CO_2/O_2 of bagasse (*line*), filter cake (*dashed line*) and vinasse (*dotted line*)

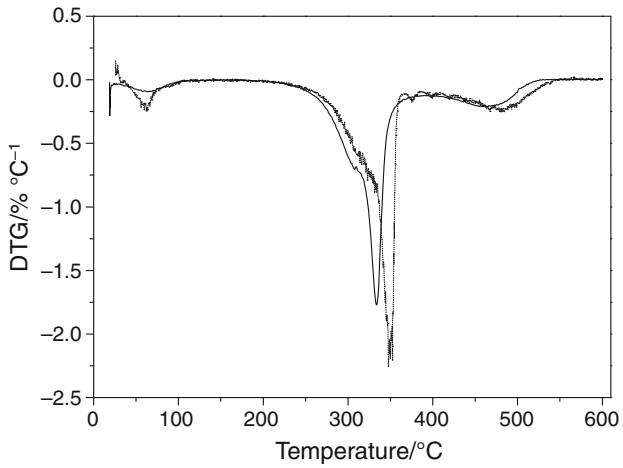

Fig. 5 DTG curves in N_2/O_2 (*line*) and CO_2/O_2 (*dotted line*) of bagasse

Similar DSC profiles were observed for each sample (Fig. 7). In the beginning, there was an endothermic peak until around 150 °C (moisture loss). Later, two exothermic shoulders emerged. The first one (180–430 °C) was related to oxidative decomposition of cellulose and hemicellulose, whereas the second one (430–above 600 °C) was associated with the degradation of lignin and char oxidation. Also, it was noticed that the second exothermic peak was, for all samples, more intense than the first. Since a high heating rate (20 °C min^{-1}) was employed for the experiments, release of volatiles at the beginning of thermal decomposition was not favored. However, there was an inducement of char oxidation which caused an increase in second peak's intensity. These events have been reported recently in a study which determined the influence of the heating rate in DSC analysis [40].

Blends showed resembling profiles (an endothermic peak followed by two exothermic shoulders) only with increased intensity than observed for original samples. Besides, there was a displacement of the second exothermic shoulders to lower temperatures when vinasse was a blend constituent. Such event, which ended above 600 °C for the original sample of vinasse, showed maximum peak intensity between 460 °C and 505 °C for the blends B + V and Fc + V.

In CO_2 atmosphere, vinasse started to decompose in lower temperatures than bagasse, as previously seen in N_2, N_2/O_2 and CO_2/O_2 (Fig. 8). However, a mass loss step between 700 and 850 °C appeared which was not observed

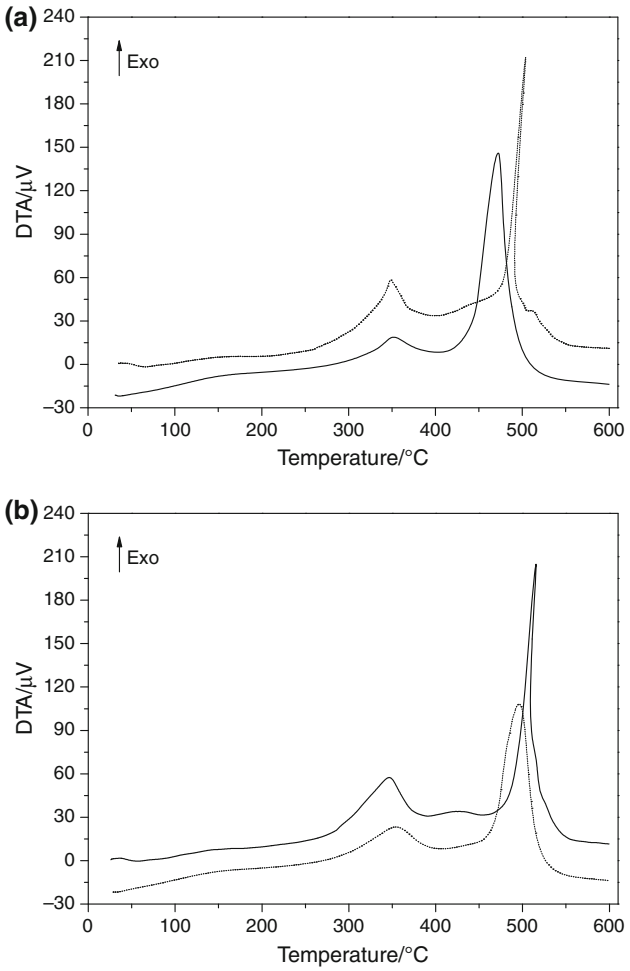

Fig. 6 DTA curves in N_2/O_2 (*line*) and CO_2/O_2 (*dotted line*) of **a** B + V and **b** Fc + V

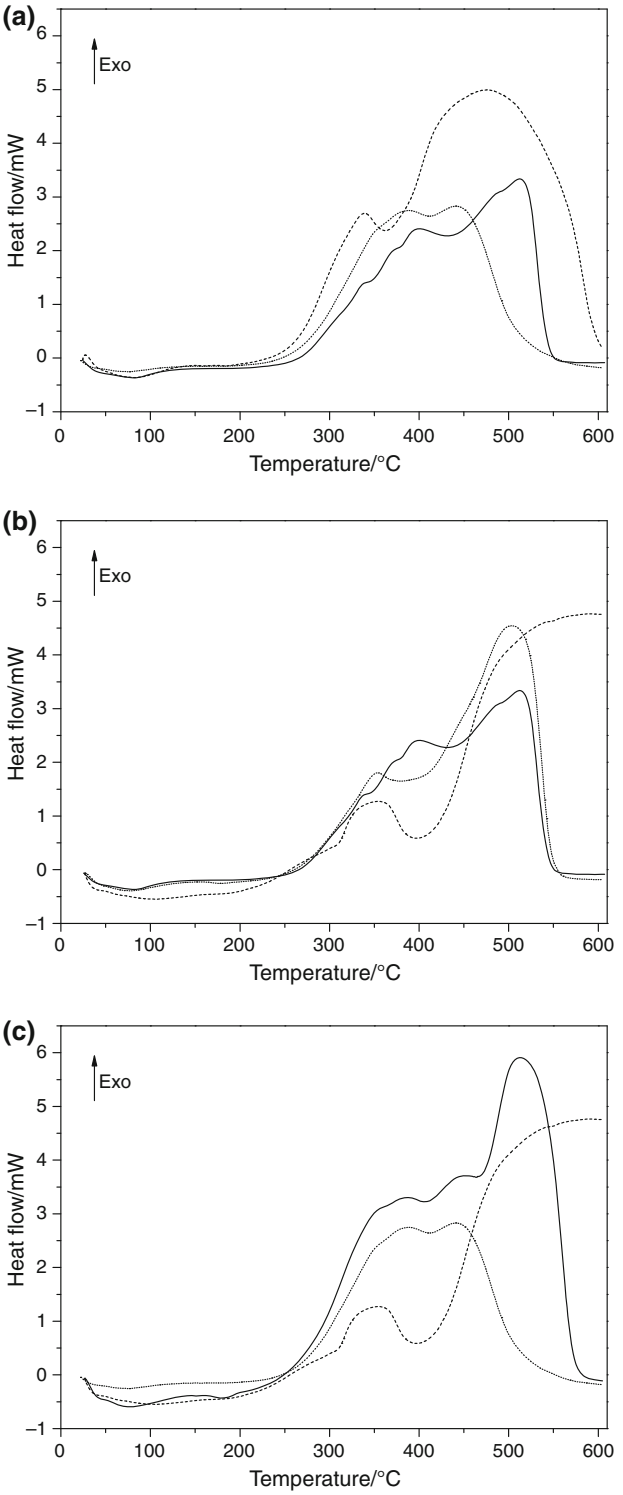

Fig. 7 DSC curves of **a** bagasse (*line*), filter cake (*dashed line*) and B + Fc (*dotted line*); **b** bagasse (*line*), vinasse (*dashed line*) and B + V (*dotted line*); **c** filter cake (*line*), vinasse (*dashed line*) and Fc + V (*dotted line*)

for bagasse. The DTA curve of vinasse showed an endothermic peak at that temperature interval.

Several works on coal gasification [24–26, 41, 42] reported that presence of alkali and alkaline earth metals (mainly potassium) catalyzed the reverse Boudouard reaction (Eq. 2), one of the most important in that process which yields CO. Boudouard equilibrium is the following:

$$C + CO_2 \rightleftharpoons 2CO \quad \Delta H = +172\,\text{kJ mol}^{-1} \tag{2}$$

This reaction is highly endothermic and produces carbon monoxide at a significant rate only at high temperatures (above 900 °C). Nevertheless, when carbonates containing such metals are present, that reaction can take place at lower temperatures ($T > 700$ °C), near fusion points of that carbonates [43].

In that catalytic process, the carbonate (K_2CO_3) is bonded to the char surface. When heated in CO_2 atmosphere, oxygen atoms of the carbonate react with surface carbon atoms producing CO and generating a reduced potassium complex. CO_2 from the atmosphere oxidizes such reduced complex forming a new complex (–COK) and releasing carbon monoxide. Around 800 °C, potassium

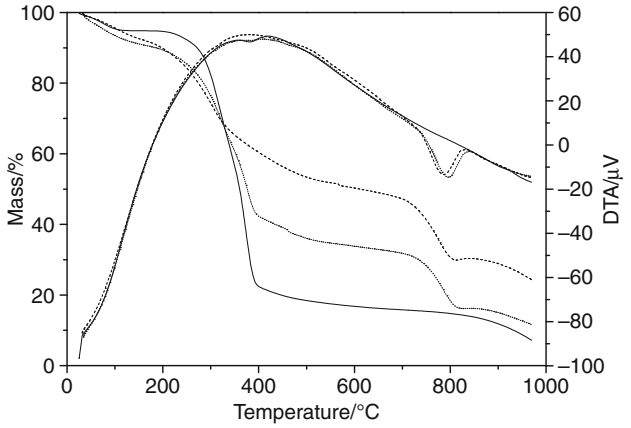

Fig. 8 TG and DTA curves for bagasse (*line*), vinasse (*dashed line*) and B + V (*dotted line*) in CO_2 atmosphere

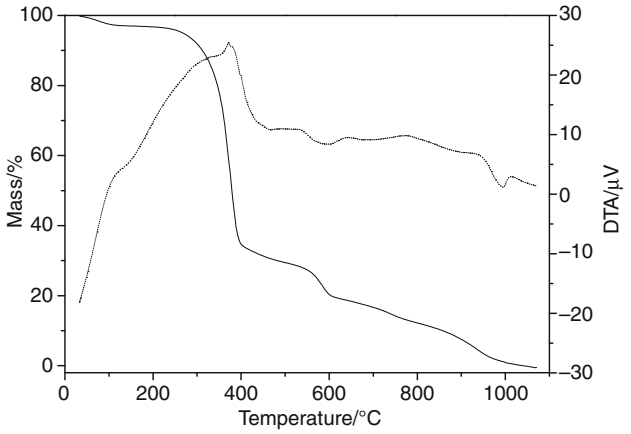

Fig. 9 TG (*line*) and DTA (*dotted line*) curves for K-enriched bagasse in CO_2 atmosphere

evaporates and the catalytic process comes to a halt [44]. Thus, due to the high potassium content detected in vinasse by flame photometry (110 g kg^{-1}), possibly a similar process could occur in that sample.

B + V blend showed an intermediate behavior in relation to the original samples. Notwithstanding, as noticed in vinasse, the blend started early to decompose in relation to bagasse and an endothermic mass loss step took place around 750 °C.

Bagasse presented a very similar trend as observed in N_2. However, at 600 °C, about 18 % of the sample still remained in CO_2, while only 5 % were detected in N_2 atmosphere. Presence of CO_2 in the environment affected the release of volatiles and, later, decomposition of the produced char resulting in a larger mass of sample at the same temperature.

When K-enriched bagasse was heated in CO_2 atmosphere (Fig. 9), it was observed the same TG profile previously detected for bagasse until around 400 °C. Then, a mass loss stage appeared and it was observed until 600 °C due, possibly, to biphthalate degradation. Finally, another mass loss stage associated with an endothermic peak was detected. This peak had low intensity and presented its apex at, approximately, 990 °C. As previously described, when the samples of vinasse and B + V blend were heated in the same conditions, we believe that a similar process occurred for K-enriched bagasse. After addition of potassium biphthalate, bagasse presented the same endothermic peak at a higher temperature than the observed for vinasse and B + V blend. Probably, such trend happened due to a lower concentration of potassium in the K-enriched bagasse sample (comparing to vinasse and B + V blend) since a 1 % potassium biphthalate solution was used for that procedure. However, more studies need to be done in order to verify such observations. Nevertheless, probably, the reverse Boudouard reaction was catalyzed after addition of potassium to bagasse.

Evaluation of synergistic effect

It was not observed noticeable changes regarding to DTG curves profiles of blends in N_2 environment as can be seen by Fig. 10a. Every studied blend presented an experimental DTG curve very resembling to the estimated one in that atmosphere.

Blends that contained bagasse presented such changes, both in synthetic air and in CO_2/O_2. When bagasse was added to filter cake, an increase in intensity of the second decomposition step peak (around 340 °C) was detected. Such increment was not estimated in both atmospheres (Fig. 10b, c). B + V blend showed, apart from a more intense peak, displacement of the third mass loss step which emerged nearly 440 °C in synthetic air and 510 °C in CO_2/O_2 (Fig. 10d, e).

These events denoted an increase in reactivity of such samples which was probably caused by higher content of volatiles belonging to bagasse. The weaker covalent bonds of those molecules cleaved yielding free radicals. When they reacted with filter cake or vinasse, the decomposition reactions were favored in a process very similar to biomass–coal blends as reported in some studies [45].

Nevertheless, Fc + V blend did not show an increase in reactivity mainly for lower volatile content compared to bagasse. Moreover, it was observed in synthetic air environment: a decrease in peak intensities referring to the first two mass loss steps (approximately 300 °C) and a displacement of the third mass loss peak (around 490 °C) to higher temperatures than estimated (Fig. 10f). Possibly, occurred retention of volatiles by inorganic compounds, present in both constituents of the blend, yielded

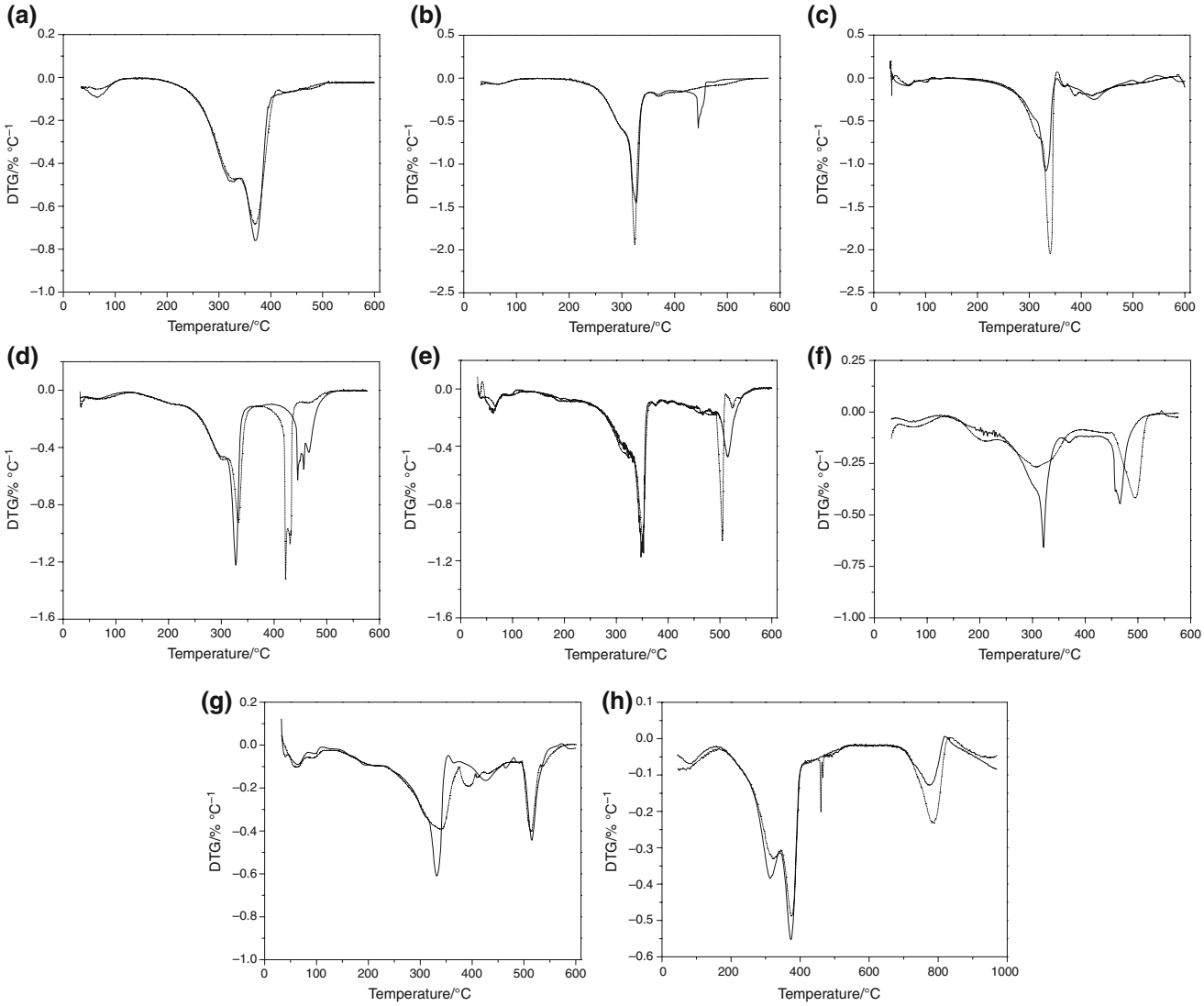

Fig. 10 Estimated (*line*) and experimental (*dotted line*) DTG curves of B + Fc in **a** N_2; **b** N_2/O_2; **c** CO_2/O_2; B + V in **d** N_2/O_2; **e** CO_2/O_2; Fc + V in **f** N_2/O_2; **g** CO_2/O_2; **h** B + V in CO_2

secondary carbonates [46] and, thereby, delayed this decomposition step. In CO_2/O_2 atmosphere was noticed some decrease in first peak intensity (around 320 °C). Still, the second peak of the experimental DTG curve presented a very like behavior of the estimated curve which denoted the absence of synergism between blend constituents (Fig. 10g).

In CO_2 atmosphere, the B + V blend showed a decrease in DTG peak intensity for the first and second decomposition steps (<400 °C) when the experimental curve profile is compared to the estimated one (Fig. 10h). However, there was a increase in intensity of the last experimental DTG peak (∼790 °C) combined with a displacement to higher temperatures of such peak (approximately, 10 °C increment).

Again, probably, the higher content of volatiles due to the addition of bagasse to vinasse played a crucial role in those events. First, the CO_2 molecules exerted a higher partial pressure on volatiles, which made their release slower in relation to the other studied atmospheres. Then, around 790 °C, a greater content of carbon was available to be converted to CO by the reverse Boudouard reaction, thus, increasing the experimental DTG peak intensity. Furthermore, despite containing half of vinasse mass and, consequently, half of potassium concentration, the DTG peak intensity of the blend was very resembling to the one detected for the vinasse sample in the same conditions (-0.232 % °C^{-1} and -0.244 % °C^{-1}, respectively) for such decomposition step. Therefore, it is very likely that the process of thermal decomposition in CO_2 atmosphere of the B + V blend is analogous to co-gasification of coal (or petroleum coke) and biomass blends [27–29].

Conclusions

When bagasse was mixed with the other samples (B + Fc and B + V), the last mass loss step began at lower temperatures when compared to Fc + V blend. A higher content of volatiles, mainly released by bagasse, reacted with the produced char and induced blend decomposition. Such observation is very resembling to the co-firing of coal–biomass or low rank–high rank coal blends, in which the blend constituent with high content of volatiles promotes char decomposition.

Displacement of mass loss steps to higher temperatures in oxy-combustion atmosphere in relation to combustion atmosphere was caused by higher heat capacity of CO_2 when compared to N_2. Furthermore, some of these steps presented a higher decomposition rate due to the increment of partial pressure associated with carbon dioxide molecules. Thus, variation of reaction atmosphere affected heat transfers and kinetics, which are relevant points regarding new technologies.

Vinasse decomposition initiated at lower temperatures than other samples in every studied atmosphere. Possibly, because of lack of fibers in its composition and different interactions between organic and inorganic matter in that sample, the thermal stability of vinasse was lower than bagasse and filter cake. Therefore, sample morphology should be taken into account since it affects directly its thermal behavior.

Although a greater heat flow was detected for all blends in relation to pure samples, only in blends with bagasse as a constituent (B + Fc and B + V) occurred synergetic interactions that favored their thermal decomposition in combustion and oxy-combustion atmospheres. Since more volatiles were present in such blends, their reactivity was increased and allowed char oxidation to take place at lower temperatures.

Probably, in CO_2 atmosphere, the reverse Boudouard reaction could have been catalyzed by potassium in vinasse. Combining such waste with a biomass rich in volatile matter (bagasse) presented an increase in reactivity in a process analogous to co-gasification of coal and biomass blends. Also, due to its higher moisture content, it could be easily mixed with other types of biomass. Hence, synergistic interactions between vinasse and other types of biomass will be evaluated on next studies.

Acknowledgements The authors are grateful to the Institute of Chemistry (IQ/CAr) of UNESP and University of São Paulo (USP). We would like to thank the sugarcane mills for providing the samples used in this work. The main author would like to acknowledge CAPES for financial support.

References

1. Adhikari DK, Seal D, Saxena C, Goyal HB. Biomass based fuel/energy. J Petrotech Soc. 2006;3(1):28–42.
2. Goyal HB, Saxena C, Seal D. Thermochemical conversion of biomass to liquids and gaseous fuels. In: Pandey A, editor. Handbook of plant-based biofuels. Boca Raton: CRC Books; 2009. p. 30–1.
3. Chen G, Andries J, Spliethoff H. Catalytic pyrolysis of biomass for hydrogen rich fuel gas production. Energy Convers Manage. 2003;44:2289–96.
4. Hansen J, Ruedy R, Glascoe J, Sato M. GISS analysis of surface temperature change. J Geophys Res. 1999;104:30997–1002.
5. Wall T, Liu Y, Spero C, Elliott L, Khare S, Rathnam R, Zeenathal F, Moghtaderi B, Buhre B, Sheng C, Gupta R, Yamada T, Makino K, Yu J. An overview on oxyfuel coal combustion—state of the art research and technology development. Chem Eng Res Des. 2009;87:1003–16.
6. Arias B, Pevida C, Rubiera F, Pis JJ. Effect of biomass blending on coal ignition and burnout during oxy-fuel combustion. Fuel. 2008;87:2753–9.
7. Toftegaard MB, Brix J, Jensen PA, Glarborg P, Jensen AD. Oxy-fuel combustion of solid fuels. Prog Energy Combust Sci. 2010;36:581–625.
8. Barnes AC. The sugar cane. London: Leonard Hill; 1964. p. 365–6.
9. Mutton MA, Rossetto R, Mutton MJR. Utilização agrícola da vinhaça. In: Cortez LAB, coordinator. Bioetanol de cana-de-açúcar: P&D para produtividade e sustentabilidade. São Paulo: Blücher; 2010, p. 423–40.
10. Ramalho JF, Amaral Sobrinho NM. Metais pesados em solos cultivados com cana-de-açúcar pelo uso de resíduos agroindustriais. Revista Floresta e Ambiente. 2001;8(1):120–9.
11. Agarwal CS, Pandey GS. Soil pollution by spent wash discharge: depletion of manganese (II) and impairment of its oxidation. J Environ Biol. 1994;15:49–53.
12. Silva MAS, Griebeler NP, Borges LC. Uso da vinhaça e impactos nas propriedades do solo e lençol freático. Revista Brasileira de Engenharia Agrícola e Ambiental. 2007;11(1):108–14.
13. Demirbas A. Fuels from biomass. In: Demirbas A, editor. Biorefineries: for biomass upgrading facilities. London: Springer; 2010. p. 33–73.
14. Cortez LAB, Silva A, Lucas J Jr, Jordan RA, Castro LR. Biodigestão de efluentes. In: Cortez LAB, Lora ES, editors. Biomassa para energia. Campinas: Editora da UNICAMP; 2007. p. 493–529.
15. González JF, García CMG, Ramiro A, González J, Sabio E, Gañán J, Rodríguez MA. Combustion optimisation of biomass residue pellets for domestic heating with a mural boiler. Biomass Bioenerg. 2004;27(2):145–54.
16. Öhman M, Boman C, Hedman H, Nordin A, Bostrom D. Slagging tendencies of wood pellet ash during combustion in residential pellet burners. Biomass Bioenergy. 2004;27(6):585–96.
17. Nussbaumer T. Combustion and co-combustion of biomass: fundamentals, technologies and primary measures for emission reduction. Energy Fuels. 2003;17:1510–21.
18. Nielsen HP, Frandsen FJ, Dam-Johansen K, Baxter LL. The implications of chlorine-associated corrosion on the operation of biomass-fired boilers. Prog Energy Combust Sci. 2000;26:283–98.
19. Backman R, Khalil RA, Todorovic D, Skreiberg O, Becidan M, Goile F, Skreiberg A, Sorum L. The effect of peat ash addition to demolition wood on the formation of alkali, lead and zinc compounds at staged combustion conditions. Fuel Process Technol. 2013;105:20–7.

20. Demirbas A. Sustainable cofiring of biomass with coal. Energy Convers Manag. 2003;44:1465–79.
21. Biagini E, Lippi F, Petarca L, Tognotti L. Devolatilization rate of biomasses and coal-biomass blends: an experimental investigation. Fuel. 2002;81:1041–50.
22. Baxter L. Biomass-coal co-combustion: opportunity for affordable renewable energy. Fuel. 2005;84:1295–302.
23. Wigmans ST, Göebel JC, Moulijn JA. The influence of pretreatment conditions on the activity and stability of sodium and potassium catalysts in carbon–steam reactions. Carbon. 1983; 21(3):291–301.
24. Veraa MJ, Bell AT. Effect of alkali metal catalysts on gasification of coal char. Fuel. 1978;57:194–200.
25. Yokoyama S, Miyahara K, Tanaka K, Takakuwa I, Tashiro J. Catalytic reduction of carbon dioxide. 1. Reduction of carbon dioxide with carbon carrying potassium carbonate. Fuel. 1979; 58:510–4.
26. Mckee DW, Spiro CL, Kosky PG, Lamby EJ. Catalysis of coal char gasification by alkali metal salts. Fuel. 1983;62(2):217–20.
27. Krerkkaiwan S, Fushimi C, Tsutsumi A, Kuchontara P. Synergetic effect during co-pyrolysis/gasification of biomass and subbituminous coal. Fuel Process Technol. 2013;115:11–8.
28. Lahijani P, Zainal ZA, Mohamed AR, Mohammadi M. CO_2 gasification reactivity of biomass char: catalytic influence of alkali, alkaline earth and transition metal salts. Bioresour Technol. 2013;144:288–95.
29. Nemanova V, Abedini A, Liliedahl T, Engvall K. Co-gasification of petroleum coke and biomass. Fuel. 2014;117:870–5.
30. Gil MV, Oulego P, Casal MD, Pevida C, Pis JJ, Rubiera F. Mechanical durability and combustion characteristics of pellets from biomass blends. Bioresour Technol. 2010;101:8859–67.
31. Lajiji M, Limousy L, Jeguirim M. Physico-chemical properties and thermal degradation characteristics of agropellets from olive mill by-products/sawdust blends. Fuel Process Technol. 2014; 1126:215–21.
32. Jirícek I, Rudasová P, Zemlová T. A thermogravimetric study of the behavior of biomass blends during combustion. Acta Polytech. 2012;52(3):39–42.
33. Jones JM, Darvell LI, Bridgeman TG, Pourkashanian M, Williams A. An investigation of thermal and catalytic behaviour of potassium in biomass combustion. Proc Combust Inst. 2007;31:1955–63.
34. Jesus HC, Costa EA, Mendonça ASF, Zandonade E. Distribuição de metais pesados em sedimentos do sistema estuarino da ilha de Vitória-ES. Quim Nova. 2004;27(3):376–86.
35. Kastanaki E, Vamvuka D, Grammelis P, Kakaras E. Thermogravimetric studies of the behavior of lignite–biomass blends during devolatilization. Fuel Process Technol. 2002;77:159–66.
36. Glória NA. Utilização agrícola da vinhaça. Brasil Açucareiro. 1975;86:11–7.
37. Bhosale PR, Chonde SG, Nakade DB, Raut PD. Studies on physic-chemical characteristics of waxed and dewaxed pressmud and its effect on water holding capacity of soil. ISCA J Biol Sci. 2012;1(1):35–41.
38. Carlson CL, Adriano DC. Environmental impacts of coal combustion residues. J Environ Qual. 1993;22:227–47.
39. Kumar R, Mago G, Balan V, Wyman CE. Physical and chemical characterization of corn stover and poplar solids resulting from leading pretreatment technologies. Bioresour Technol. 2009;100: 3948–62.
40. Chen H, Liu N, Fan W. Two-step consecutive reaction model of biomass thermal decomposition by DSC. Acta Physicochim Sin. 2006;22(7):786–90.
41. Sutton D, Kelleher B, Ross JRH. Review of literature on catalysts for biomass gasification. Fuel Process Technol. 2001;73:155–73.
42. Vamvuka D, Karouki E, Sfakiotakis S, Salatino P. Gasification of waste biomass chars by carbon dioxide via thermogravimetry—effect of catalysts. Combust Sci Technol. 2012;184(1):64–77.
43. Mckee DW, Chatterji D. The catalytic effect of alkali metal carbonates and oxides in graphite oxidation reactions. Carbon. 1975;13:381–90.
44. Kopyscinski J, Rahman M, Gupta R, Mims CA, Hill JM. K_2CO_3 catalysed CO_2 gasification of ash-free coal. Interactions of the catalyst with carbon in N_2 and CO_2 atmosphere. Fuel. 2014;117: 1181–9.
45. Edreis EMA, Luo G, Li A, Chao C, Hu H, Zhang S, Gui B, Xiao L, Xu K, Zhang P, Yao H. CO_2 co-gasification of lower sulphur petroleum coke and sugar cane bagasse via TG-FTIR analysis technique. Bioresour Technol. 2013;136:595–603.
46. Haas J, Tamura M, Weber R. Characterization of coal blends for pulverised fuel combustion. Fuel. 2001;80:1317–23.